Drug Design, Development and Therapy

Dovepress
open access to scientific and medical research

Open Access Full Text Article

ORIGINAL RESEARCH

SIRT1/FOXO1 Axis-Mediated Hippocampal Angiogenesis is Involved in the Antidepressant Effect of Chaihu Shugan San

Shan Zhang[1], Yujia Lu[1], Wei Shi[1], Yi Ren[1], Kaihui Xiao[1], Wei Chen[2], Li Li[1], Jingjie Zhao[1,3]

[1]Department of Traditional Chinese Medicine, Beijing Friendship Hospital, Capital Medical University, Beijing, 100050, People's Republic of China; [2]Experimental and Translational Research Center, Beijing Friendship Hospital, Capital Medical University, Beijing, 100050, People's Republic of China; [3]Department of Integrated Traditional and Western Medicine, Capital Medical University, Beijing, 100050, People's Republic of China

Correspondence: Jingjie Zhao, Beijing Friendship Hospital, Capital Medical University, No. 95 Yong-an Road, Beijing, 100050, People's Republic of China, Tel/Fax +86 10-63139096, Email zhaojj@ccmu.edu.cn

Objective: Chaihu Shugan San (CSS) has a long history for treating major depressive disorder (MDD), which has been verified effectively and safely in clinical studies. Deficient angiogenesis plays important roles in MDD. However, the underlying mechanisms of CSS on angiogenesis remain poorly understood.

Methods: Network pharmacology analysis was applied to explore the potential angiogenic targets and pathways between CSS and MDD. These targets would be validated in chronic unpredictable mild stress (CUMS)-induced depressive-like mice by Western blots, immunofluorescence, and immunohistochemistry. Then, the underlying molecular mechanisms were further investigated in brain microvascular endothelial cells (BMVECs) with CSS-containing serum by Western blots and immunofluorescence.

Results: Network pharmacology analysis showed that the antidepressant role of CSS was closely associated with Silent information regulator protein 1 (SIRT1)/Forkhead box O1 (FOXO1) axis-mediated angiogenesis. This prediction was confirmed in the following experiments. CSS induced angiogenesis, increased SIRT1 expression, and decreased FOXO1 expression in the hippocampus of CUMS mice. Five percent CSS-containing serum produced a significant increase in BMVECs proliferation, migration, and tube formation, but these effects were reduced by SIRT1 silencing. CSS serum could also promote FOXO1 translocation to the cytoplasm through SIRT1 signaling, which triggered FOXO1 protein degradation. What is more, CSS upregulated VEGFA and BDNF expressions not only in the hippocampus of depressive mice but also in BMVECs supernatants. Of note, these trophic factors play important roles in promoting neurogenesis.

Conclusion: The study showed that CSS could promote angiogenesis and neurogenesis in the hippocampus of CUMS-induced mice. The underlying molecular mechanism involves the SIRT1/FOXO1 axis and subsequent regulation of VEGFA and BDNF. These findings provide novel insight into CSS drug development, and targeting the SIRT1/FOXO1 axis might be a promising strategy to treat MDD.

Keywords: major depressive disorder, Chaihu Shugan San, SIRT1/FOXO1 axis, angiogenesis, brain microvascular endothelial cell

Introduction

Major depressive disorder (MDD) is a serious mental disorder, characterized by a high incidence, diverse symptoms, complex etiologies, and unclear pathological mechanisms.[1] In currently clinical practice, traditional antidepressants were not effective to all patients; only 40–60% of patients respond to antidepressant therapy, among which approximately one third achieve remission and 30% may occur treatment resistance although receiving optimal antidepressant treatment according to consensus guidelines.[2] Furthermore, these antidepressants usually cause some side effects including gastrointestinal side effects, blurred vision, sexual problems, etc.[3,4] Compared with traditional antidepressant drugs, the antidepressant effect of ketamine is obvious and quick. However, ketamine does not present an ideal profile as an antidepressant due to its potential psychotomimetic effects as well as abuse potential.[5,6] Besides, other antidepressant

Received: 14 April 2022
Accepted: 12 August 2022
Published: 23 August 2022

Graphical Abstract

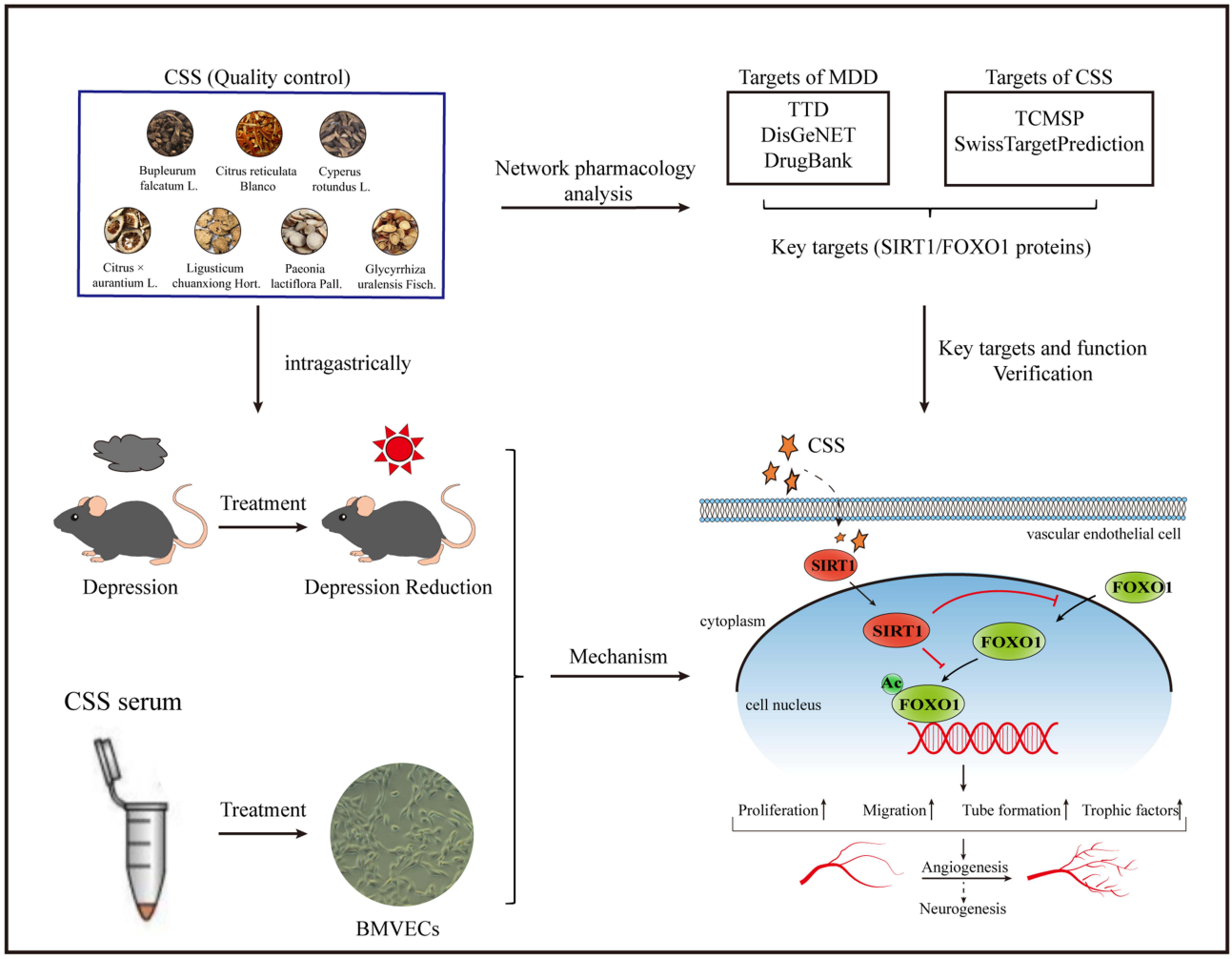

treatments such as psychotherapy and repetitive transcranial magnetic stimulation (rTMS) also have a certain curative effect but they also have some adverse effects or limitations. For example, the most common adverse effects for rTMS are scalp pain during stimulation (~40%) and transient headache after stimulation (~30%).[7] Psychotherapy, relatively non-invasive to patients, is recommended to treat mild depression.[8] Therefore, there is a constant need to develop novel antidepressants with greater efficacy, fewer side effects for MDD treatment, which has become a focus of research in recent years.

Chaihu Shugan San (CSS) is a classical traditional Chinese medicine (TCM) formula that is used clinically to treat depression in China. Evidence from meta-analysis studies revealed that CSS can effectively and safely improve depressed symptoms in MDD patients.[9–11] Study showed that the efficacy of CSS was significantly better than antidepressants in reducing Hamilton Depression Rating Scale (HDRS) score and lightly increasing effective rate (65.1% VS 58.2%).[9] More importantly, CSS was associated with less adverse events than antidepressants, such as anxiety, reduced/ increased appetite, dry mouth, constipation.[10,11] Currently, increasing numbers of studies are endeavoring to explore the underlying mechanisms of CSS. Some studies have shown that CSS can stimulate adult neurogenesis and upregulate the expression of brain-derived neurotrophic factor (BDNF) in rats with depression-like behaviors.[12,13] Of note, microvessels are an important medium to provide nutrients for nerve survival, growth, and differentiation.

Moreover, CSS induced anti-atherosclerotic effects and improved depression-like behaviors in mice with coronary heart disease. Interestingly, the upregulation of BDNF in endothelial cells is possibly involved in this process.[14] Clinical study found that CSS treatment could significantly increase the regional cerebral blood flow and decrease the depressive symptoms in patients, which was nearly the same as Fluoxetine.[15] These above studies indicated that the antidepressant roles of CSS were associated with brain microvessels. However, the effects of CSS on brain microvessels and the involved mechanisms have not been investigated.

Angiogenesis plays an important role in depression. Some studies have reported that decreased vessel density was observed in depressed patients.[16–18] Furthermore, vascular endothelial growth factor (VEGF) and BDNF acted as important pro-angiogenic factors and were decreased in depressed patients and stressed mice.[19–21] One study also showed that the angiogenesis inhibitor (VEGF receptor inhibitor, SU1498) blocked the angiogenic effect of exercise (non-pharmacological treatment) on stressed mice.[22] Collectively, it is reasonable to speculate that angiogenesis is involved in the pathogenesis of depression, but this needs to be further confirmed and explored.

Silent information regulator protein 1 (SIRT1), a nicotinamide adenine dinucleotide-dependent deacetylase, is abundantly expressed in vascular endothelial cells.[23] It can modulate angiogenesis through deacetylating downstream Forkhead boxo1 (FOXO1). Study revealed that resveratrol, a SIRT1 agonist, promoted wound healing via SIRT1-dependent pro-angiogenic effects and the inhibition of FOXO1 expression.[24] SIRT1 has been extensively studied for its connection to depression. A recent genome-wide association study with Han Chinese sample has identified two genetic loci for depression in SIRT1.[25] Yet, the role of SIRT1 in depression remains unclear, especially in hippocampal angiogenesis.

In the present study, we mainly used chronic unpredictable mild stress (CUMS) mouse models, network pharmacology approaches, and brain microvascular endothelial cells (BMVECs) to investigate the potential mechanisms of CSS on hippocampus angiogenesis in MDD. We aimed to provide a rationale for the use of CSS as a potential therapeutic drug for MDD treatment.

Materials and Methods

Network Pharmacology Analysis

The compounds of CSS were obtained from the Traditional Chinese Medicine System Pharmacology Database and Analysis Platform (TCMSP, http://tcmspnw.com/, updated on May 31, 2014) by retrieving herb names (ex: Bupleurum falcatum L/chai hu/柴胡) in CSS. As suggested by the TCMSP, oral bioavailability ≥ 30% and drug likeness ≥ 0.18 were used as criteria to filter the bioactive compounds of CSS. In total, there were 116 components of CSS were acquired (Table S1, Supplementary File). Then, we transformed the active compounds into canonical SMILES by the PubChem database (https://pubchem.ncbi.nlm.nih.gov/). After that, we uploaded the SMILES structures into the SwissTargetPrediction database (http://www.swisstargetprediction.ch/, updated in 2019) for CSS target prediction. Species were selected as "Homo sapiens" with probability >0 as the screening condition. The targets of MDD involving human proteins were obtained from the Therapeutic Target Database (https://db.idrblab.org/ttd/, updated on June 1, 2020), DisGeNET database (http://www.disgenet.org/web/DisGeNET/, updated in May 2020), and DrugBank database (http://www.drugbank.ca/, released on April 22, 2020), using the keywords "major depressive disorder", "depression", or "unipolar depression". "score" ≥ mean value was used as the criterion for screening disease target genes. Then, the overlapped targets of compounds in CSS and MDD were obtained for the further analyses. Finally, 147 overlapping targets were identified (Table S2, Supplementary File).

The Database for Annotation, Visualization, and Integrated Discovery (DAVID, http://david.abcc.ncifcrf.gov/, updated in October 2016) provides systematic and comprehensive biological function annotation information for multiple genes. We introduced the targets of CSS for MDD treatment into DAVID and defined the species as "Homo sapiens" for Gene Ontology (GO) analyses. A value of $p < 0.05$ was considered statistically significant. Functions related to angiogenesis were selected and further explored. Next, the interactive relationships among the predicted targets related to angiogenesis were retrieved using the Search Tool for the Retrieval of Interacting Genes/Proteins database (https://string-db.org/, updated on August 12, 2021). "Organism" was set as "Homo sapiens" and the "combined score" ≥0.4 was selected as the threshold.

The visualization process was carried out with Cytoscape v3.7.0 software. The NetworkAnalyzer plug-in in this software was applied to mine the hub targets by calculating the node degree (number of the first interacting neighbors). What's more, targets with a high degree of connectivity were selected as hub genes.

Animals

Forty male C57BL/6 mice and 20 male Sprague–Dawley rats, aged 6–8 weeks, were purchased from Beijing Vital River Laboratory Animal Technology Company (Beijing, China). All animals were housed in a humidity- and temperature-controlled environment and had free access to food and water unless otherwise indicated. The animal study followed the National Institutes of Health guide for the care and use of Laboratory animals, and approved by Experimental Animal Ethics Committee of Beijing Friendship Hospital (Grant No. 21–1008).

Drug Preparation

CSS comprises seven traditional herbal medicines, including *Bupleurum falcatum* L. (Chai-hu, 18 g), *Cyperus* × *aurantium* L. (Xiang-fu, 18 g), *Ligusticum chuanxiong* Hort. (Chuan-xiong, 18 g), *Citrus reticulata* Blanco (Chen-pi, 18 g), *Citrus* × *aurantium* L. (Zhi-qiao, 18 g), *Paeonia lactiflora* Pall. (Bai-shao, 30 g), and *Glycyrrhiza uralensis* Fisch. (Gan-cao, 10 g). CSS granules were purchased from Beijing Tcmages Pharmaceutical Company (Beijing, China). According to the conversion ratio between mice and humans (ratio, 9: 1), the daily CSS dose (g/kg) for each mouse can be calculated as the following formula: 9 × a daily dose of an adult (130 g herb)/average weight of adults (60 kg) =19.5 g herb/kg.

Serum containing drugs was prepared as previously described.[26] Ten rats in each group were randomly assigned to the control (CON)-containing serum and CSS-containing serum groups. The dosage for rats was 13.5 g herb/kg according to the conversion ratio between rats and human (ratio, 6.25: 1). The rats in the CSS-containing serum group were administered CSS (13.5 g herb/kg) by gavage once a day for 10 days, and rats in the CON group were given distilled water. Two hours after the final dose, the rats were sacrificed. Serum was collected, passed through a 0.22 μm filter, and stored at −80 °C until use.

Quality Control of CSS and CSS-Containing Serum

CSS and CSS-containing serum quality was determined by high performance liquid chromatography/mass spectrometry. The information of reference substance in CSS were provided in Table S3, Supplementary File. Weighed standards were dissolved in methanol. CSS granules were dissolved in water (0.1 g/mL), vortexed for 30 min, and centrifuged at 14000 rpm for 10 min. Serum samples were also prepared. Then, the samples were separated on an Agilent Zorbax XDX C18 phase column (50 mm × 2.1 mm × 3.5 μm, Santa Clara, CA, USA). The gradient elution solutions consisted of mobile phase A (acetonitrile) and mobile phase B (0.1% formic acid aqueous solution). The gradient elution program was as follows: 0–0.5 min 20% B; 0.5–4 min 20–80% B; 4–5 min 80% B; 5–5.01 min 80–20% B; 5.01–6 min 20% B. The flow rate was 0.5 mL/min. The column temperature was 30 °C, and a 1 μL aliquot of solution was injected.

Mass spectrometry measurements were performed on a Sciex API 4000 Qtrap MS system equipped with a Turbo Ionspray interface (Applied Biosystems, Foster City, CA, USA). Samples were analyzed in positive electrospray ionization mode or negative electrospray ionization mode and monitored in the multiple reactions monitoring mode. High purity nitrogen was used as the curtain gas, ion source gas 1, and ion source gas 2, with flow rates of 10 psi, 55 psi, and 55 psi, respectively. The spray voltage was ± 4.5 kV, and the capillary temperature was 500 °C.

CUMS Procedure and Drug Administration

Mice were randomly separated into three groups: the CON group (not subjected to CUMS and CSS), the CUMS group (subjected to CUMS), and the CUMS+CSS group (subjected to CUMS and CSS). The CUMS and CUMS+CSS groups were individually housed and underwent a 6-week CUMS procedure, which was performed as previously described.[27] Briefly, mice were randomly subjected to one long-term stressor and one short-term stressor at different times of the day. Long-term stressors mainly included overnight exposure to damp sawdust, lights on overnight, 24 h of food deprivation, 24 h of water deprivation, 24 h of exposure to wet bedding, and 45° cage tilt for 24 h. Short-term stressors included 10

min of tail pinch, 10 min of mice scream, and 2 h of restraint. The same stressor was not applied consecutively for 2 days. CON group mice were group-housed and briefly handled daily in the housing room. During this period, the CUMS +CSS group was treated with CSS (19.5 g herb/kg) by oral gavage once a day. The CON and CUMS groups were given distilled water at an equal volume. For bromodeoxyuridine (BrdU) staining, mice were intraperitoneally injected with BrdU (50 mg/kg) (No. B5002-250MG, Sigma, MO, USA) once per day for 7 days prior to the beginning of behavioral tests.

Behavioral Tests

The sucrose preference test was used to assess stress-induced anhedonia.[28] Mice were adapted to the presence of two water bottles placed in each cage for 3 days. After adaptation, the water and food were removed for 12 h. Then a bottle containing pure water and a bottle with 2% sucrose solution were presented in the cage simultaneously, and the mice had free access to these bottles for the next 24 h. Bottles were weighed to estimate the consumption of the liquids. The sucrose preference (percentage of the sucrose solution consumed relative to the total amount of liquid intake) was calculated.

Antidepressant activity was also assessed by the tail suspension test (TST). Each mouse was suspended 30 cm above the floor by the tail via tape at approximately 1 cm from the tip of the tail. The test was conducted for 10 min.[29] The immobility time, which is indicative of helpless behavior, was recorded.[30]

In the forced swim test (FST), the mice swam in an open glass beaker (height 18.5 cm and diameter 14.5 cm) filled with water (23–25 °C) up to a height of 12 cm to prevent the mice from supporting themselves against the bottom of the beaker. The mice were subjected to a 10-min session to evaluate depressive behavior and were judged as immobile whenever they remained floating passively in the water.[31]

Tissue Collection and Preparation

After the behavior tests, the anesthetized mice were transcardially perfused with saline to wash away the blood. Some tissue samples were immediately frozen in optimal cutting temperature compound and stored at –80 °C to prepare frozen sections.[32] Cryopreserved tissues were then cut into 10 μm cryosections, starting from the anterior hippocampus. Eight brain sections per animal were collected at 90-μm distances between sections for nonoverlapping multistage random sampling.[33] Other mouse hippocampus was used for Western blots.

Western Blots

The samples were extracted with radio immunoprecipitation assay buffer, and the protein concentration was determined by a bicinchoninic acid assay. Proteins were separated by 10% sodium dodecyl sulfate-polyacrylamide gel electrophoresis and blotted onto nitrocellulose membranes. The blots were blocked with 5% skim milk in tris-buffered saline and tween 20 buffer. Two hours later, the membranes were incubated overnight at 4 °C with primary antibodies including SIRT1 (1:1000, ab12193, Abcam, Cambridge, UK), FOXO1 (1:500, sc-374427, Santa, Japan), acetylated FOXO1 (1:100, MBS9600633, MyBioSource, CA, USA), VEGFA (1:1000, ab1316, Abcam, Cambridge, UK), or BDNF (1:1000, ab108319, Abcam, Cambridge, UK). After washing with tris-buffered saline tween 20 buffer, the membranes were incubated with corresponding secondary antibodies (1:5000, ab8245 or 8226, Abcam, Cambridge, UK) for 2 h at room temperature. The blots were visualized with a Bio-Rad imaging system (California, USA) and quantified using Image J software (National Institutes of Health, Bethesda, MD, USA). All protein expression was normalized to that of GAPDH or β-ACTIN.

Immunofluorescence

The sections were dried on a slide warmer for 30 min, fixed with 4% paraformaldehyde for 10 min, and permeabilized with 0.2% Triton-X100 for 10 min. Then, the sections were incubated in 2 N HCl at 37 °C for 1 h and blocked for 2 h with 5% donkey serum at room temperature. Subsequently, the slices were incubated with anti-GLUT1 (1:200, ab40084, Abcam, Cambridge, UK), anti-NeuN (1:200, ab209898, Abcam, Cambridge, UK), anti-CD34 (1:100, ab81289, Abcam, Cambridge, UK) or anti-BrdU (1:200, ab6326, Abcam, Cambridge, UK) antibodies at 4 °C overnight. After washing, the sections were incubated with the following corresponding secondary antibodies: anti-mouse or rabbit antibody-Alexa Fluor 488 (1:400,

ab150105, ab150077, Abcam, Cambridge, UK), anti-rat antibody-Cy3 (1:400, ab98416, Abcam, Cambridge, UK), or anti-rabbit antibody-Alexa Fluor 647 (1:400, ab150075, Abcam, Cambridge, UK). 4′,6-Diamidino-2-phenylindole (DAPI) was used as a nuclear counterstain. Images were obtained with a fluorescence microscope (Olympus, Tokyo, Japan). The number of positive cells was counted at 10× magnification, eight fields were sampled for each brain section, and 10 brain sections were analyzed per animal.[34] Four biological replicates were performed.

Cultured cells were fixed with 4% paraformaldehyde, permeabilized with 0.2% Triton X-100, and blocked with 5% donkey serum. Cells were incubated overnight at 4 °C with primary antibodies against SIRT1 (1:200) and FOXO1 (1:200). Either an Alexa Fluor-488 (1:200) or −594 (1:200, ab150116, Abcam, Cambridge, UK) conjugated antibody against the respective IgG was used as the secondary antibody. DAPI was used to stain cell nuclei.

Immunohistochemistry

Frozen sections were fixed with 4% paraformaldehyde for 10 min and permeabilized with 0.2% Triton-X100 for 10 min. Then, the sections were blocked for 1 h with goat serum at room temperature and incubated overnight at 4 °C with SIRT1 (1:100), FOXO1 (1:50), or GLUT1 (1:100) antibodies. Subsequently, the sections were incubated with secondary goat-anti-mouse or rabbit IgG antibodies for 1 h at room temperature. Staining was visualized with diaminobenzidine, and sections were counterstained with hematoxylin.

Mouse BMVECs Culture

In order to further verify the angiogenic roles of CSS, BMVECs culture are used in the following experiments.[35,36] BMVECs obtained from Procell (Wuhan, China) were cultured in Dulbecco's modified Eagle's medium (Sigma, MO, USA) supplemented with 10% fetal bovine serum (Sigma, MO, USA) at 37 °C in a humidified incubator (5% CO_2, 95% air). All experiments were conducted on cell lines with passage number 1 to 10.

Gene Knockdown by Small Interfering RNA (siRNA) and Cell Treatment

SIRT1 siRNA or negative control siRNA (siB14212112732-1-5 or RUIBO, SiN0000001-1-5, Guangzhou, China) were transfected at a final concentration of 50 nM using Lipofectamine RNAiMAX (13778150, Invitrogen, USA) according to the manufacturer's instructions.

To verify the proangiogenic effects of CSS, BMEVCs were treated with 5% CSS-containing serum or 5% control rat serum. To further evaluate the role of CSS in promoting angiogenesis through SIRT1/FOXO1 axis, we co-transfected 50 nM SIRT1 siRNA with 5% CSS-containing serum or 5% control rat serum into BMVECs.

CCK8 Proliferation Assay

Cells were incubated with CCK8 solution (CK04-500T, DongRen, Shanghai, China) for 2 h and assessed using a microplate reader. The optical density was quantified at 450 nm, and the cell viability (%) was calculated as follows: treatment group optical density/CON group optical density × 100%.

Scratch Assay

Cells were inoculated in six-well plates at a density of 1×10^6 cells per well. When the cells became confluent, a scratch was made in the cell monolayer with a pipette tip. The cells were photographed using an inverted microscope (Leica, Germany) at 0 and 12 h of incubation. The relative migration distance (relative migration distance = initial scratch width − the scratch width of the cells at 12 h) was assessed using Image J software.

Tube Formation Assay

Cultured cells were seeded at a cell density of 2×10^5 cells per well in a 48-well plate coated with 150 μL of growth factor-reduced Matrigel (352428, Corning, NY, USA). After 12 h of incubation, the capillary-like formations of BMVECs were photographed using an inverted microscope and quantitated by Image J software.

Nuclear and Cytoplasmic Protein Extraction

Nuclear and cytoplasmic proteins were extracted using a Nuclear and Cytoplasmic Protein Extraction Kit (P0028, Beyotime, Shanghai, China). Briefly, cells were resuspended in 200 μL of cytoplasmic protein isolation solution A and homogenized on ice for 15 min. Next, 10 μL of cytoplasmic protein isolation solution B was added, and the cells were homogenized on ice. The homogenate was centrifuged at 13000 rpm for 5 min at 4 °C. The supernatant consisted of the cytoplasmic protein fraction. The pellet was resuspended in 50 μL of nuclear protein isolation solution C, homogenized on ice, and centrifuged at 13 000 rpm for 10 min. The supernatant consisted of the nuclear protein fraction.

Enzyme-Linked Immunosorbent Assay Analysis

Cell culture medium was collected after SIRT1 siRNA transfection with or without CSS-containing serum. The BDNF and VEGFA concentrations were assayed using commercial enzyme-linked immunosorbent assay kits (CSB-E04505m or CSB-E04756m, CUSABIO, Wuhan, China) based on the kit instructions.

Statistical Analysis

Statistical analysis was performed using SPSS 22.0. Data are expressed as the mean ± standard deviation. Comparisons were performed using one-way analysis of variance, followed by Tukey's multiple comparisons test. A value of $p < 0.05$ was considered statistically significant.

Results

Quality Control of Representative Compounds in CSS and CSS-Containing Serum

A chromatogram of CSS and drug-containing serum is shown in Figure S1, Supplementary File. The following representative ingredients of CSS were detected: paeoniflorin, liquiritin, ferulic acid, naringin, hesperidin, neohesperidin, glycyrrhizic acid ammonium salt, saikosaponin A, nobiletin, saikosaponin D, tangeretin, and α-cyperone. The concentrations of ingredients are shown in Table S4, Supplementary File. The samples met the quality control criteria of the Chinese Pharmacopeia (2020 edition).

CSS Improved Depressive Behaviors in CUMS Mice

A timeline of experimental procedures is depicted in Figure 1A. Systemic treatment of CUMS mice with a dosage of 19.5 g herb /kg/day of CSS improved the depressive-like behaviors. As shown in Figure 1B and C, the CUMS mice exhibited significant decrease in body weight and sucrose preference, which are typical characteristics of depression.[37] However, CSS treatment significantly affected the changes in body weight and sucrose preference, with mice exhibiting levels similar to those of the CON group. CUMS mice exhibited an increased immobility time in the TST and FST compared with the CON mice ($p < 0.01$; $p < 0.01$), but CSS treatment ameliorated these effects ($p < 0.05$, $p < 0.01$, Figure 1D and E). These results indicated that CSS had a clear antidepressant effect in CUMS mice.

Hippocampal Angiogenesis is Involved in the Antidepressant Effects of CSS

Network pharmacology analysis was performed to further investigate the possible mechanisms underlying the antidepressant-like effects of CSS treatment. As shown in Figure 2A, 147 potential shared targets for antidepressant activity were found between CSS and MDD. The functional enrichment analysis results were closely associated with angiogenesis. The biological functions mainly included angiogenesis, vasoconstriction, endothelial cell proliferation, regulation of VEGFs, cell migration, and sprouting. Among these functions, angiogenesis was the top and most notable biological process involved in CSS-treated MDD (Figure 2B). Subsequently, double immunofluorescence staining for BrdU (newborn cell marker) and GLUT1 (vascular endothelial marker) was used to evaluate angiogenesis in the three groups. Chronic exposure decreased the generation of newborn vascular endothelial cells in the CUMS mouse hippocampus, as $GLUT1^+/BrdU^+$ cells in the CUMS group were significantly reduced compared with those in the CON group ($p < 0.01$). Conversely, administration of CSS to CUMS mice significantly increased the number of $GLUT1^+/BrdU^+$ cells in the hippocampus, indicating that CSS alleviated the CUMS-induced decrease in angiogenesis ($p < 0.05$, Figure 2C and D).

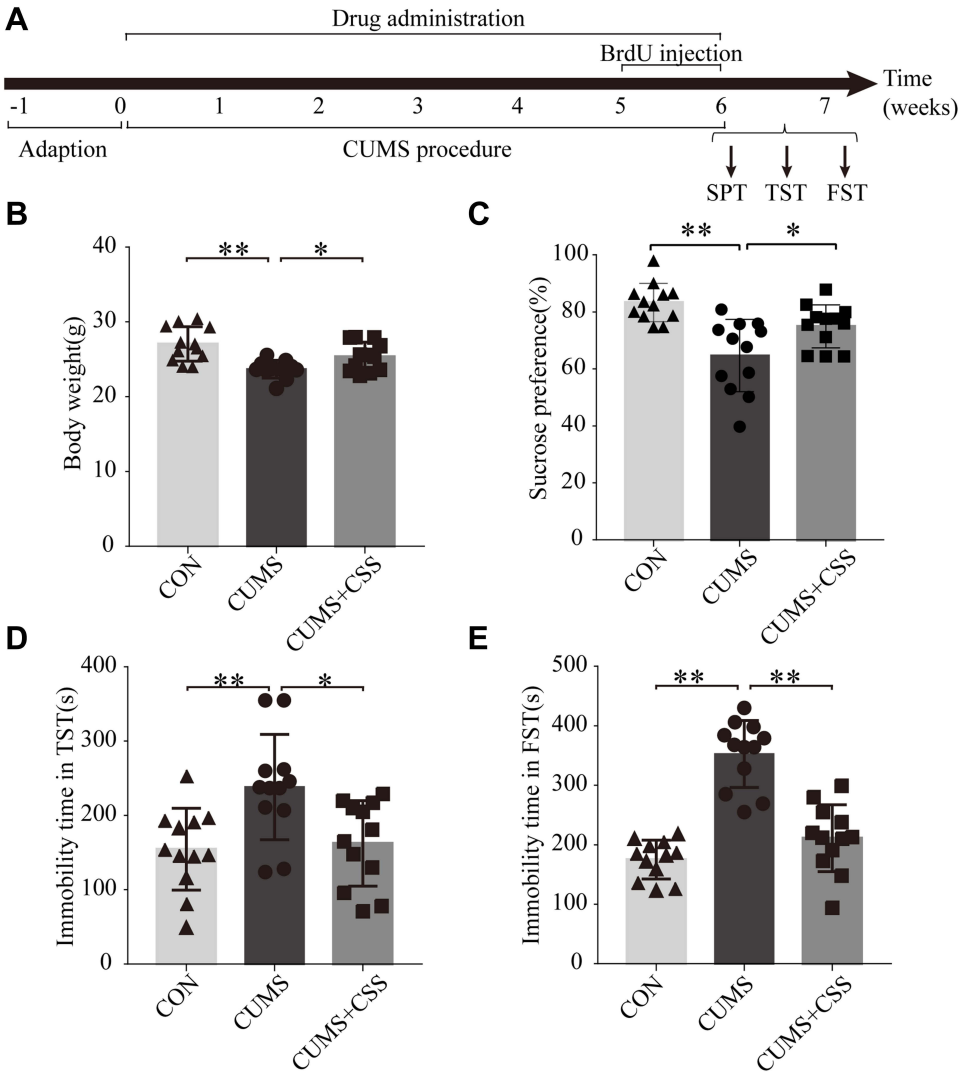

Figure 1 CSS improved depressive behaviors in CUMS mice. (**A**) The timeline of experimental procedures. (**B**–**E**) Behavioral tests were performed to confirm the antidepressant effect after CSS treatment. The bodyweight (**B**), sucrose preference test (**C**), tail suspension test (TST) (**D**), forced swim test (FST) (**E**) among three groups were evaluated. Data are expressed by mean ± SEM (n=12). Asterisk represents statistically significant difference (*$p < 0.05$, **$p < 0.01$).

Consistent with the above results, the number of $CD34^+/BrdU^+$ cells (another newborn vascular endothelial marker) also decreased in the hippocampus of CUMS mice compared with CON mice, and CSS treatment could partly reverse this change (Figure 2, Supplementary File). Compared with the CUMS group, the numbers of $BrdU^+$ cells were increased in the CON and CUMS+CSS groups ($p < 0.01$, $p < 0.05$, Figure 2C and E). In summary, these results indicated that hippocampal angiogenesis is involved in the antidepressant effects of CSS.

SIRT1/FOXO1 Axis-Mediated Hippocampal Angiogenesis is Involved in the Antidepressant Effects of CSS in CUMS Mice

We further explored the hub genes that participate in angiogenesis through network pharmacological analysis. Protein-protein interaction network analysis showed that SIRT1 and FOXO1 exhibited high degrees among the targets and dominated the network (Figure 3A). SIRT1 expression in the hippocampus was significantly decreased in CUMS mice but was increased after CSS treatment ($p < 0.05$, $p < 0.01$, Figure 3B and C). FOXO1 and acetylated FOXO1 expression levels were significantly increased in CUMS mice compared with the CON group ($p < 0.05$), whereas their expression levels were exhibited near-normal levels with CSS treatment ($p < 0.05$, Figure 3B, D and E). Immunohistochemical

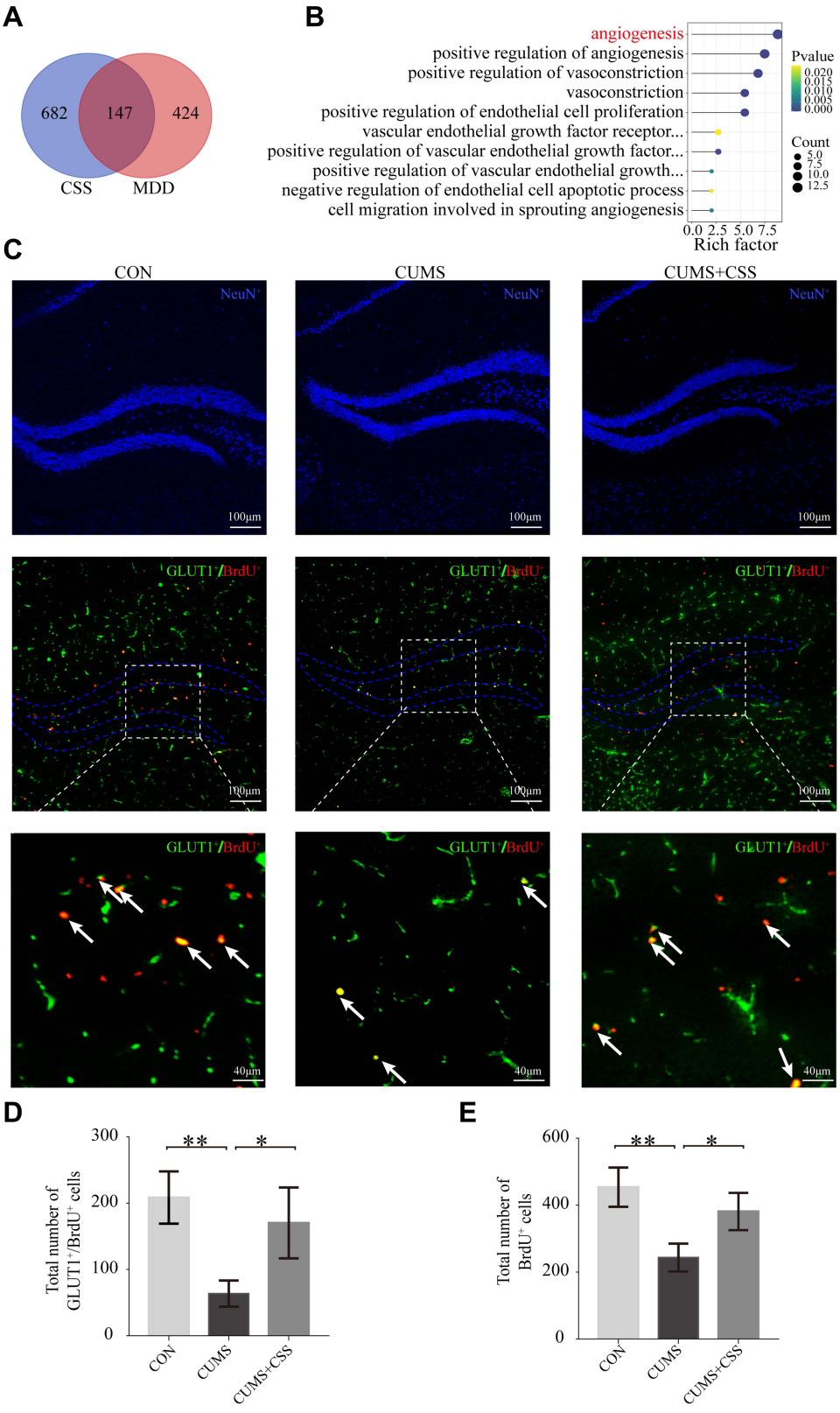

Figure 2 The antidepressive effects of CSS were closely associated with angiogenesis. (**A**) Network pharmacological analysis showed that there were 147 overlapping targets between CSS and MDD. (**B**) Biological process analysis of the overlapped targets shared by CSS and MDD. Functions associated with angiogenesis was selected. Size and color of the bubble represent the number of genes enriched in the biological process and statistical significance, respectively. The Y axis represents the function term, the X axis represents the rich factor (rich factor= amount of differentially expressed genes enriched in the pathway/amount of all genes in background). (**C**) Confocal images to show the distribution and cell number of $GLUT1^+/BrdU^+$ cells in hippocampus. Newborn cells and endothelial cells labeled by BrdU (red) and GLUT1 (green) in hippocampus respectively. White arrows indicate the newborn endothelial cells. Quantification of $GLUT1^+/BrdU^+$ cells (**D**), total $BrdU^+$ cells (**E**) in hippocampus of CUMS mice treated with vehicle or CSS. Data are expressed by mean ± SEM (n=3). Asterisk represents for statistically different (*$p < 0.05$, **$p < 0.01$).

https://doi.org/10.2147/DDDT.S370825 DovePress

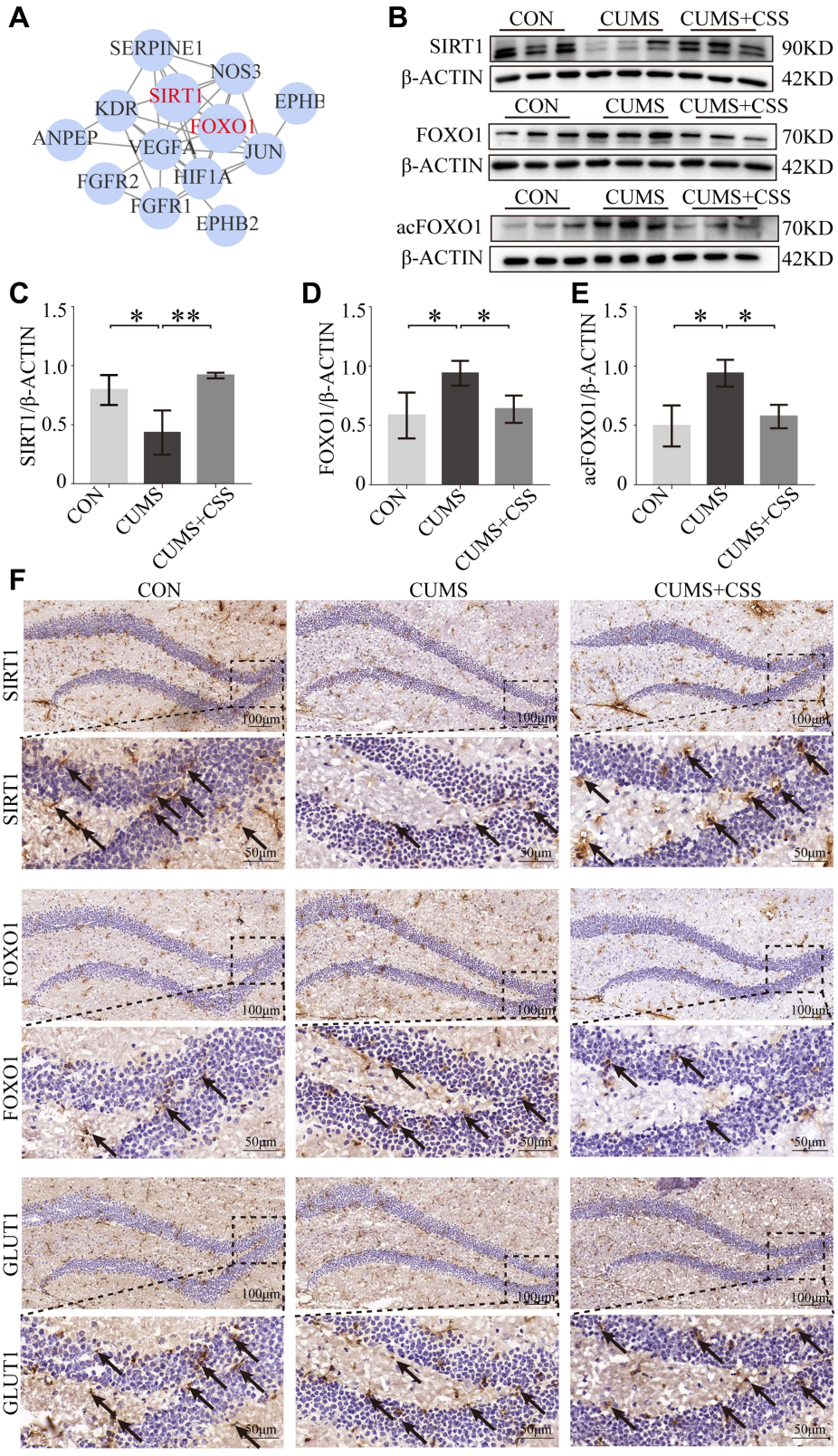

Figure 3 SIRT1/FOXO1 axis mediated angiogenesis is involved in the antidepressant effects of CSS. (**A**) The protein-protein interaction network of the targets associated with the biological process of angiogenesis. Nodes represent targets, lines represent the connections between targets. (**B**) Representative Western blots images show the effects of CSS on SIRT1/FOXO1 axis in CUMS mice with CSS treatment or not. (**C**) SIRT1, (**D**) total FOXO1, (**E**) ac-FOXO1 were quantified. β-ACTIN was used as inner reference. (**F**) Immunohistochemical staining of SIRT1, FOXO1 and GLUT1 protein in hippocampus among three groups (×200 and ×600). Black arrows indicate the positive signals. Data are expressed by mean ± SEM (n=3). Asterisk represents a statistical difference (*$p < 0.05$, **$p < 0.01$).

analysis also confirmed the Western blotting findings. As shown in Figure 3F, SIRT1 and GLUT1 expression showed a decreased trend, but FOXO1 was obviously increased in the hippocampus of CUMS mice, and CSS treatment prevented these changes. Of note, SIRT1 and FOXO1 proteins were partly found in hippocampal endothelial cells. It is likely that CSS treatment promotes shuttling of FOXO1 protein into the cytoplasm, accelerating FOXO1 protein degradation.

CSS-Containing Serum Promoted BMVECs Proliferation, Migration, and Tube Formation by Targeting SIRT1

Dose- and time-dependent CCK8 experiments confirmed that treatment with 5% CSS-containing serum for 12 h could achieve a peak effect on BMVECs proliferation (Figure 4A and B). Therefore, 5% CSS-containing serum were adopted for subsequent cell experiments. Target-specific siRNA was employed in BMVECs to verify the role of SIRT1 protein in CSS-induced angiogenic activities. As shown in Figure 4C and D, CSS-containing serum promoted BMVECs proliferation at 6 h and 12 h, but this effect was attenuated in the si-SIRT1+CSS group ($p < 0.01$). Migration of BMVECs was significantly enhanced after CSS serum treatment for 12 h compared with the CON serum group ($p < 0.01$). However, SIRT1 knockdown significantly abolished the enhancement of CSS-induced BMVECs migration ($p < 0.01$, Figure 4E and F). A tube formation assay was performed to detect cell tube formation capabilities. As shown in Figure 4G–J, addition of 5% CSS-containing serum resulted in a significant increase in mesh formation and branching lengths ($p < 0.05$), and a slight increase in the number of nodes in BMVECs, but the effect was neutralized by SIRT1-specific siRNA treatment. Taken together, these results indicated that CSS can promote BMVECs angiogenesis via targeting SIRT1 protein.

FOXO1, as a Downstream Molecule of SIRT1, Participates in the Pro-Angiogenic Effects of CSS-Containing Serum

We further explored the downstream effectors of SIRT1 in BMVECs in vitro. As shown in Figure 5A–D, SIRT1 inhibition in BMVECs upregulated FOXO1 and acetylated FOXO1 in groups with or without CSS-containing serum treatment ($p < 0.01$). FOXO1 expression was also detected in the nucleus and cytoplasm to further assess its activation (Figure 5E–G). Cytoplasmic FOXO1 expression was higher in the CSS serum group than in the CON serum group, whereas SIRT1 siRNA could abolish this effect ($p < 0.05$). Conversely, nuclear FOXO1 expression was lower in the CSS serum group than in the CON serum group. This inhibition was also obviously abrogated by SIRT1 knockdown ($p < 0.01$). Notably, FOXO1 in the nucleus exhibited high transcriptional activity and reduced angiogenesis. We subsequently analyzed the subcellular localization of SIRT1 and FOXO1 by immunofluorescence staining (Figure 5H). SIRT1 was mainly localized in the nucleus, while FOXO1 was distributed in the cytoplasm after co-incubation with CSS-containing serum, which is consistent with the Western blotting results. However, the CSS serum-mediated cytoplasmic distribution of FOXO1 was abolished in siRNA-SIRT1 transfected BMVECs. In all, these results clearly demonstrated that CSS exerted angiogenic effects that were dependent on the SIRT1/FOXO1 axis.

CSS Promoted Neurotrophic Factor Expression and Secretion, Which Might Benefit Neurogenesis

As shown in Figure 6A–C, BDNF and VEGFA protein expression levels have a significantly decreased trend in the hippocampus of CUMS mice, which could be upregulated by CSS treatment ($p < 0.05$, Figure 6A–C). We further investigated whether suppression of SIRT1 influenced the neurotrophic factors expression or secretion in BMVECs. The Western blotting results shown in Figure 6D–F further confirmed this point. SIRT1 si-RNA decreased BDNF and VEGFA expression in BMVECs with CSS-containing serum treatment. Additionally, compared with the CON serum group, the VEGFA and BDNF contents in the cell culture supernatants were significantly increased by treatment with CSS-containing serum ($p < 0.05$). In SIRT1-deficient BMVECs, CSS-containing serum did not increase the content of these nutritional factors ($p < 0.01$, $p < 0.05$, Figure 6G and H). We further observed neurogenesis in the hippocampus of CUMS mice with CSS treatment. $NeuN^+/BrdU^+$ and $GlUT1^+/BrdU^+$ cells were simultaneously markedly decreased in CUMS mice compared with CON mice, while this effect was prevented by CSS treatment. These results indicated that

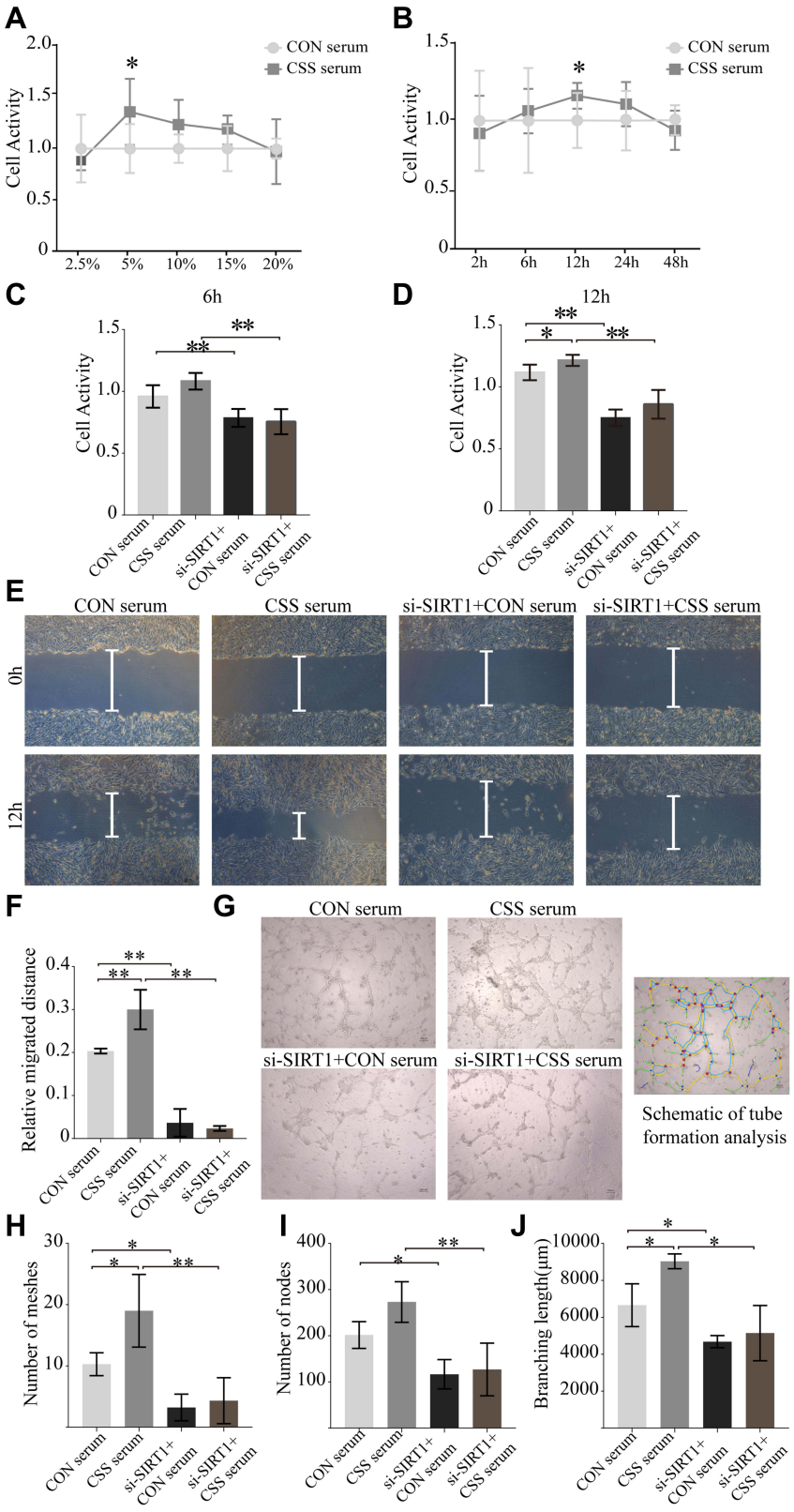

Figure 4 CSS promote angiogenic activities of endothelial cells by targeting SIRT1. (**A**) The proliferative capacity of BMVECs in different concentrations of CSS-containing serum from 2.5% to 20% at 12h. (**B**) The proliferative capacity of BMVECs with 5% CSS-containing serum at 2h, 6h, 12h, 24h, 48h. (**C** and **D**) The role of SIRT1 in the CSS-induced proliferative activities at 6h and 12h. (**E**) Representative images showing BMVECs migration at 12h (n=6). (**F**) Quantitative analysis of the migration distance in scratch assay. (**G**) Representative images showing BMVECs tube formation. Images were taken at 12 h. The blue circles represent the meshes; the pink and yellow dots represent the nodes; the lines represent branches. Quantitative analysis of number of meshes (**H**), number of nodes (**I**) and branching lengths (**J**) in tube formation assay. Data are expressed by mean ± SEM (n=3). *$p < 0.05$, and **$p < 0.01$.

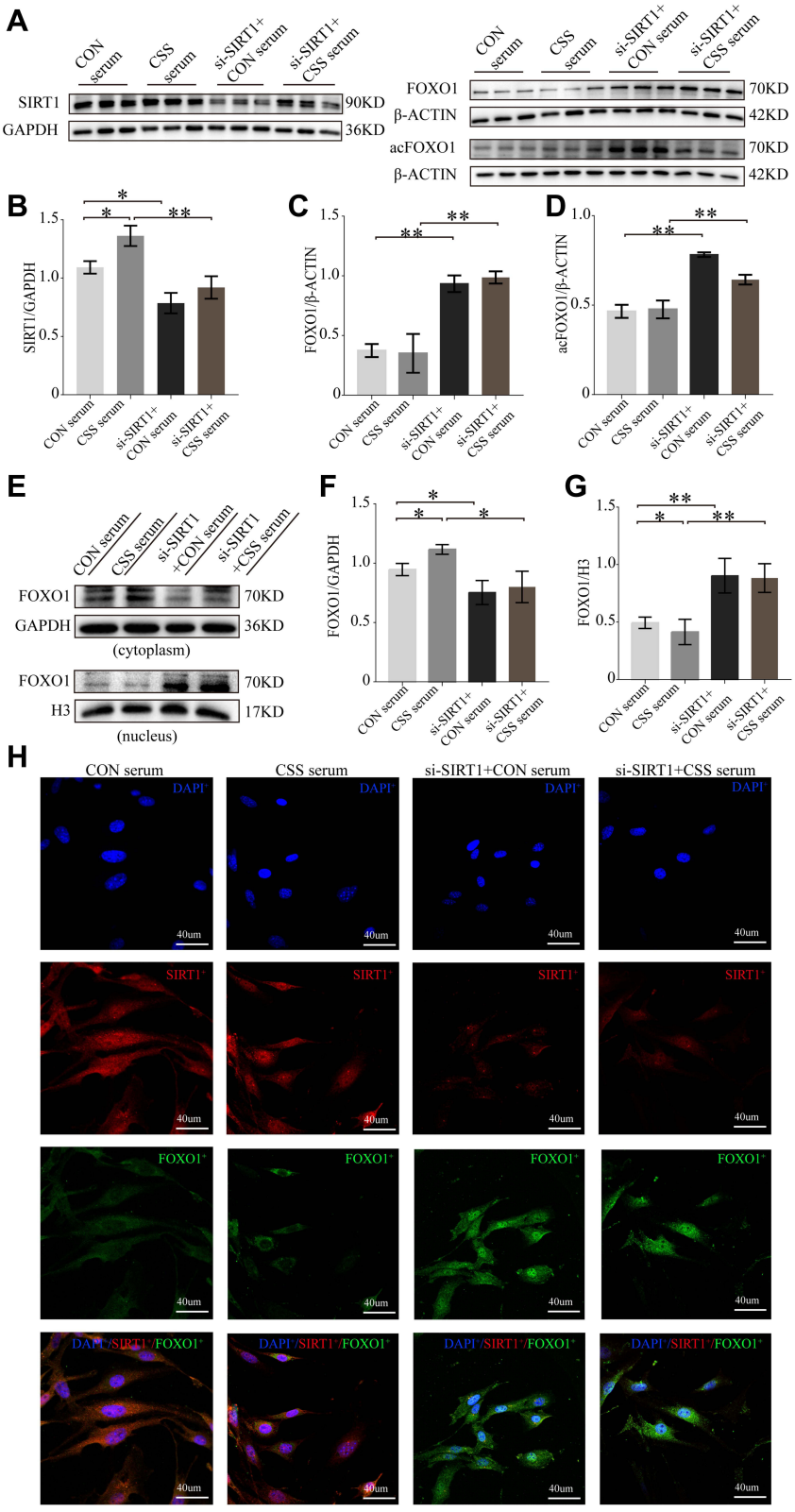

Figure 5 FOXO1, as a downstream molecule of SIRT1, participates in the pro-angiogenic effects of CSS- containing serum. (**A**) Cell lysates of BMVECs were used to detect the SIRT1, FOXO1, and acFOXO1 protein levels by Western blotting. The quantitative analysis of SIRT1 (**B**), FOXO1 (**C**), acFOXO1 (**D**). (**E**) Cytosolic FOXO1 and nuclear FOXO1 protein levels were detected by Western blots. Quantitative analysis of cytosolic FOXO1 (**F**), nuclear FOXO1 (**G**). (**H**) Representative immunofluorescence with SIRT1 and FOXO1 in BMVECs (×600). SIRT1 showed red fluorescence, FOXO1 showed green fluorescence. DAPI is blue and represents the nuclear signal. Data are expressed by mean ± SEM (n=3). Asterisk represents a statistical difference (*$p < 0.05$; **$p < 0.01$).

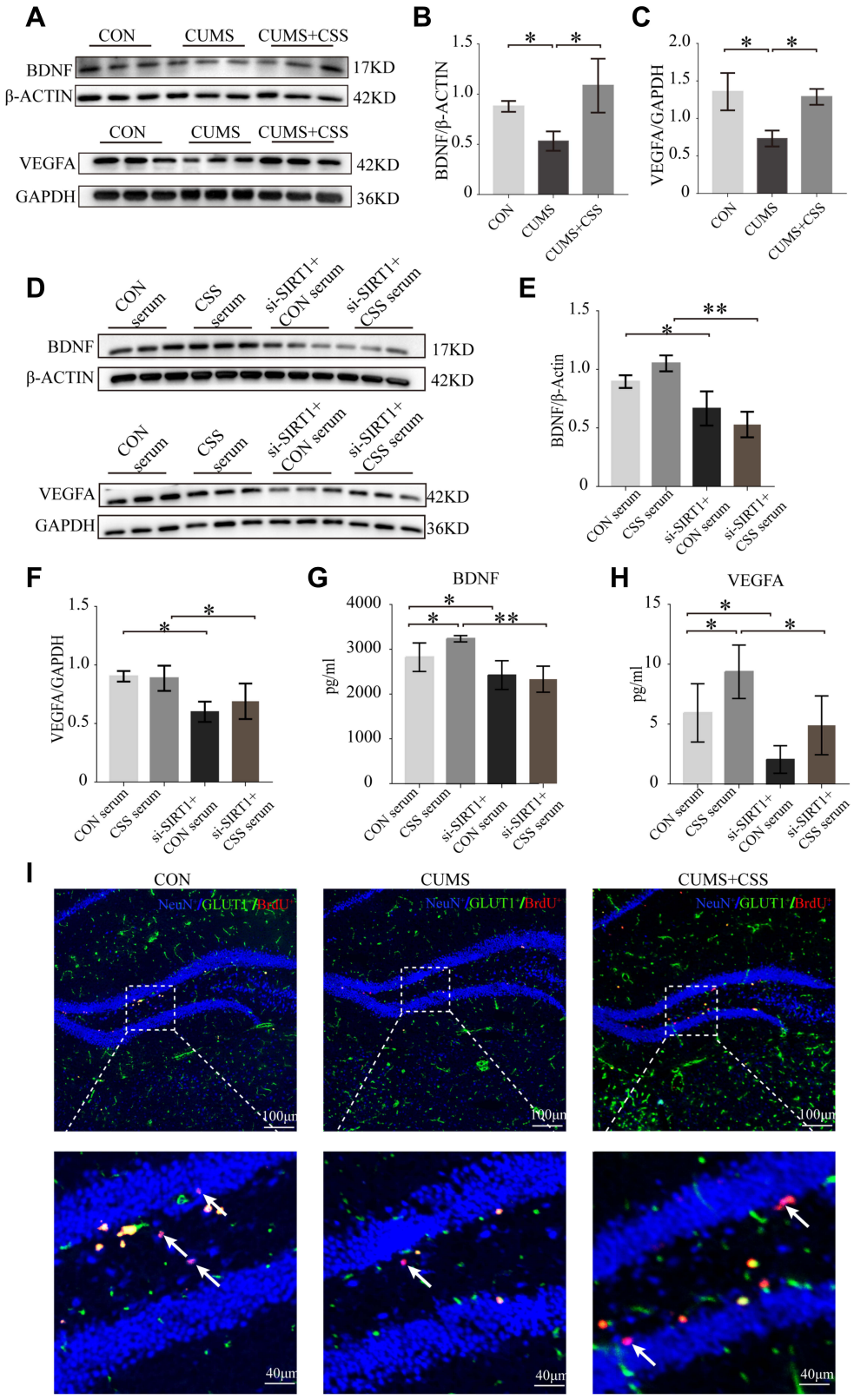

Figure 6 CSS promoted the expression or secretion of neurotrophic factors, which might facilitate neurogenesis. (**A**) BDNF and VEGFA expression in hippocampus were detected by Western blotting. The quantitative analysis of BDNF protein (**B**) and VEGFA protein (**C**) in hippocampus. (**D**) BDNF and VEGFA expression were detected in BMVECs by Western blotting. The quantitative analysis of BDNF protein (**E**) and VEGFA protein (**F**) in BMVECs. (**G** and **H**) The content of BDNF and VEGFA in cell culture supernatant were detected by enzyme-linked immunosorbent assay analysis (n=5). (**I**) Confocal images to show the distribution and cell number of $GLUT1^+/BrdU^+$ cells and $NeuN^+/BrdU^+$ in hippocampus. Newborn endothelial cells were labeled by BrdU (red) and GLUT1 (green); newborn neurons were labeled by BrdU (red) and NeuN (blue). White arrows indicate the newborn neurons (n=3). Asterisk represents a statistical difference (*$p < 0.05$; **$p < 0.01$).

CSS or CSS serum treatment could promote neurotrophic factors expression /secretion in the hippocampus of CUMS mice or BMVECs, which might promote neurogenesis.

Discussion

CSS is a classic TCM, widely used in the clinical treatment of MDD in China. Previous studies have reported that treatment of depression with CSS involves several biological aspects, such as anti-inflammatory effects, hypothalamic-pituitary-adrenal axis regulation, neurotransmitter reuptake inhibition, and promotion of neurogenesis.[38–40] However, because of the complex bioactive compounds in CSS, its exact mechanisms require in-depth study to expand its clinical applications for MDD. Our present study provides strong evidence for CSS as a potent therapeutic drug for MDD. The results showed that CSS improved anhedonia and behavioral despair in CUMS mice, which was consistent with previous studies.[41,42] In addition, in the high-performance liquid chromatography/mass spectrometry analysis, Saikosaponin A in *Bupleurum falcatum* L., naringin, hesperidin, and neohesperidin in *Citrus reticulata* Blanco and *Citrus* × *aurantium* L., paeoniflorin in *Paeonia lactiflora* Pall., ferulic acid in *Ligusticum chuanxiong* Hort., and liquiritin and glycyrrhizic acid ammonium salt in *Glycyrrhiza uralensis* Fisch. were identified as the main compounds in CSS. This result will assist in the quality control of CSS and will contribute to determining the potential roles of these compounds.

Network pharmacology analysis establishes a "compound-protein/gene-disease" network, which was suitable for mining the underlying relationships across complex disease, therapeutic targets, and multiple compounds in TCM.[43] The results suggested that CSS-induced antidepressant effects were tightly related to angiogenesis. Studies reported that depressive patients or animals revealed abnormal expression of angiogenic genes or proteins, such as VEGFR2, endoglin.[44–46] Transcriptome analysis by RNA-seq in dentate gyrus cells of postmortem in MDD patients also showed evidence of upregulated anti-angiogenic genes.[47] Clinical finding showed that increased angiogenesis was associated with a better response to antidepressant treatment. Electroconvulsive seizure induced a strong angiogenesis in the hippocampus.[48] VEGFA, as a pro-angiogenic factor, has recently been described as mimicking the actions of antidepressants and as having the potential to enhance the treatment response to conventional antidepressants.[49] Whereas, the results of clinical trials using the angiogenesis inhibitors interferon-α and belimumab found an increase in the incidence of depressive symptoms among treated participants.[50,51] In the present study, we found that CSS treatment could increase the number of new microvessels in the hippocampus of CUMS mice. This result provided key evidence for the induction of angiogenesis by CSS treatment in CUMS mice. Therefore, targeting angiogenic genes or proteins may be a valuable strategy to improve anti-depression therapy.

Angiogenesis is a complex process regulated by multiple signaling pathways. Therein, SIRT1 is a vital target that can deacetylate FOXO1, thus attenuating the FOXO1-induced inhibitory effects on angiogenesis. Studies have found that targeting SIRT1 signaling promoted angiogenesis alleviated cerebral ischemic injury,[52] improved diabetic wound healing,[24] and alleviated arthritis.[53] Our network pharmacology analysis showed that SIRT1 and FOXO1 protein dominated in the protein-protein interaction network, implying that this pathway plays an important role in the antidepressant role of CSS. Therefore, it is of great significance to explore the mechanism by which CSS promotes angiogenesis in depression by affecting these targets. Our experiments found that SIRT1 and FOXO1 protein were mainly expressed in vascular endothelial cells. CSS increased SIRT1 expression, decreased FOXO1 and acFOXO1 expressions. We used SIRT1 siRNA for reverse verification to verify the above experimental results, to some extent, it indicated that CSS could promote angiogenesis by targeting SIRT1/FOXO1 axis. Furthermore, SIRT1 controls the nuclear shuttling of FOXO1 depending on different cellular and environmental stimuli.[54,55] Particularly, in vascular endothelial cells, FOXO1 has high transcriptional activity in the nucleus and regulates downstream related targets, such as VEGFA, c-MYC, and CD36, thus limiting angiogenesis.[56–58] In our present study, CSS serum promoted FOXO1 shuttling from the nucleus to the cytoplasm, reducing FOXO1 expression and inducing angiogenesis activity. These results suggest that the mechanism by which CSS promotes angiogenesis is closely related to the upregulation of SIRT1 expression. Targeting SIRT1 protein might be a promising therapeutic target in MDD treatment. Study has demonstrated that pharmacologic or genetic ablation of hippocampal SIRT1 resulted in an elevation in depression-like behavior in mice.[59] Whereas, resveratrol, a potent SIRT1 activators, has a good antidepressant-like effects in depressed mice.[60] Therefore, activating SIRT1 may open new perspectives for the development of natural compounds as therapeutic drugs towards MDD treatments.

Neurogenesis is inextricably linked to angiogenesis. Neural stem cells exist in neurovascular niches where endothelial cells provide direct cell contacts and secrete neurotrophic factors, such as VEGFA, BDNF.[61] Studies have shown that the release or expression of VEGFA and/or BDNF significantly increases in neurogenesis in hippocampus and alleviates depressive behaviors in mice.[20] Our results also confirmed that CSS upregulated VEGFA and BDNF expressions not only in the hippocampus of depressive mice, but also in BMVECs supernatants. These results implied that CSS promoted neurotrophic factor expression and secretion, which were beneficial for neurogenesis. This process induces coordination of endogenous angiogenesis and neurogenesis, which contributes to improving depression. Our study observed this phenomenon which might associated with the SIRT1/FOXO1 axis. However, it was a preliminary study. More research is required to under the angiogenic mechanisms of CSS in CUMS mice. The deep molecular mechanisms of angiogenesis and neurogenesis are worthy of further exploration.

Conclusion

The present study demonstrated that CSS could improve depressive-like behaviors in CUMS mice, which might be caused by enhanced angiogenesis via the SIRT1/FOXO1 axis. The in vitro results showed that CSS could stimulate BMVECs proliferation, migration, and tube formation, and increase neurotrophic factors expression and secretion. However, these effects could be reduced by SIRT1 silencing. This study provides new insights into the clinical application of CSS and enhances our understanding of the mechanisms of depression.

Abbreviations

BDNF, Brain-derived neurotrophic factor; BMVECs, Brain microvascular endothelial cells; BrdU, Bromodeoxyuridine; CSS, Chaihu Shugan San; CON, Control; CUMS, Chronic unpredictable mild stress; DAPI, 4′,6-Diamidino-2-phenylindole; DAVID, Database for Annotation, Visualization, and Integrated Discovery; FOXO1, Forkhead box O1; FST, Forced swim test; GLUT1, Glucose transporter-1; MDD, Major depressive disorder; rTMS, repetitive transcranial magnetic stimulation; siRNA, small interfering RNA; SIRT1, Silent information regulator protein 1; TCM, traditional Chinese medicine; TCMSP, Traditional Chinese Medicine System Pharmacology Database and Analysis Platform; TST, Tail suspension test; VEGF, Vascular endothelial growth factor.

Data Sharing Statement

The data that support the finding of the present study are shown in Supplementary Materials.

Ethics Approval

The study was approved by Experimental Animal Ethics Committee of Beijing Friendship Hospital (Grant No. 21-1008).

Acknowledgments

This study was supported by the National Natural Science Foundation of China (Grant No. 82004109) and the Beijing Natural Science Foundation (Grant No. 7204250). We are grateful to Prof. Feng Qiu of Capital Medical University for his support in the high-performance liquid chromatography/mass spectrometry analysis. We also thank Lisa Kreiner, PhD, from Liwen Bianji, (Edanz), for editing the English text of a draft of this manuscript.

Author Contributions

All authors made a significant contribution to the work reported, whether that is in the conception, study design, execution, acquisition of data, analysis and interpretation, or in all these areas; took part in drafting, revising or critically reviewing the article; gave final approval of the version to be published; have agreed on the journal to which the article has been submitted; and agree to be accountable for all aspects of the work.

Disclosure

The authors report no conflicts of interest in relation to this work and declare that the research was conducted in the absence of any commercial or financial relationships that can be construed as a potential conflict of interest.

References

1. Malhi GS, Mann JJ. Depression. *Lancet*. 2018;392(10161):2299–2312. doi:10.1016/s0140-6736(18)31948-2
2. Anthony C, Pariante CM, Young AH, et al. Evidence-based guidelines for treating depressive disorders with antidepressants: a revision of the 2008 British Association for Psychopharmacology guidelines. *J Psychopharmacol*. 2015;29(5):4590525. doi:10.1177/0269881115581093
3. Vincenzo O, Matteo L, Riccardo P, et al. Gastrointestinal side effects associated with antidepressant treatments in patients with major depressive disorder: a systematic review and meta-analysis. *Prog Neuro*. 2021;109:110266. doi:10.1016/j.pnpbp.2021.110266
4. Alessandro S, Alberto C. Treatment-emergent sexual dysfunction related to antidepressants: a meta-analysis. *J Clin Psychopharmacol*. 2009;29 (3):259–266. doi:10.1097/JCP.0b013e3181a5233f
5. Elizabeth DB, Carlos AZ. The role of dissociation in ketamine's antidepressant effects. *Nat Commun*. 2020;11:6431. doi:10.1038/s41467-020-20190-4
6. Newport DJ, Schatzberg AF, Charles BN. Whither ketamine as an antidepressant: Panacea or Toxin? *Depress Anxiety*. 2016;33(8):685–688. doi:10.1002/da.22535
7. Roumen VM, Peter G, Sidney HK, et al. Canadian Network for Mood and Anxiety Treatments (CANMAT) 2016 clinical guidelines for the management of adults with major depressive disorder: section 4. Neurostimulation treatments. *Can J Psychiatry*. 2016;61(9):561–575. doi:10.1177/0706743716660033
8. Pim C, Soledad Q, Christopher D, et al. Psychological treatment of depression in primary care: recent developments. *Curr Psychiatry Rep*. 2019;21 (12):129. doi:10.1007/s11920-019-1117-x
9. Jin WD, Xing BP, Wang HQ, et al. Meta-analysis of clinical efficacy of chaihu shugansan in treatment of depression. *Chin Archiv Tradi Chin Med*. 2009;27(07):1397–1399. doi:10.13193/j.archtcm.2009.07.54.jinwd.024
10. Yeung WF, Chung KF, Ng KY, Yu YM, Ziea ET, Ng BF. A systematic review on the efficacy, safety and types of Chinese herbal medicine for depression. *J Psychiatr Res*. 2014;57:165–175. doi:10.1016/j.jpsychires.2014.05.016
11. Wang Y, Fan R, Huang X. Meta-analysis of the clinical effectiveness of traditional Chinese medicine formula Chaihu-Shugan-San in depression. *J Ethnopharmacol*. 2012;141(2):571–577. doi:10.1016/j.jep.2011.08.079
12. Chen XQ, Li CF, Chen SJ, et al. The antidepressant-like effects of Chaihu Shugan San: dependent on the hippocampal BDNF-TrkB-ERK/Akt signaling activation in perimenopausal depression-like rats. *Biomed Pharmacother*. 2018;105:45–52. doi:10.1016/j.biopha.2018.04.035
13. Yan L, Xu X, He Z, et al. Antidepressant-like effects and cognitive enhancement of coadministration of Chaihu Shugan San and fluoxetine: dependent on the BDNF-ERK-CREB signaling pathway in the hippocampus and frontal cortex. *Biomed Res Int*. 2020;2020:2794263. doi:10.1155/2020/2794263
14. Li L, Yu AL, Wang ZL, et al. Chaihu-Shugan-San and absorbed meranzin hydrate induce anti-atherosclerosis and behavioral improvements in high-fat diet ApoE(-/-) mice via anti-inflammatory and BDNF-TrkB pathway. *Biomed Pharmacother*. 2019;115:108893. doi:10.1016/j.biopha.2019.108893
15. Qiu J, Hu SY, Shi GQ, Wang SE. Changes in regional cerebral blood flow with Chaihu-Shugan-San in the treatment of major depression. *Pharmacogn Mag*. 2014;10(40):503–508. doi:10.4103/0973-1296.141775
16. Yamada MK. Angiogenesis in refractory depression: a possible phenotypic target to avoid the blood brain barrier. *Drug Discov Ther*. 2016;10 (2):74–78. doi:10.5582/ddt.2016.01003
17. Almeida OP, Ford AH, Flicker L, et al. Angiogenesis inhibition and depression in older men. *J Psychiatry Neurosci*. 2014;39(3):200–205. doi:10.1503/jpn.130158
18. Boldrini M, Hen R, Underwood MD, et al. Hippocampal angiogenesis and progenitor cell proliferation are increased with antidepressant use in major depression. *Biol Psychiatry*. 2012;72(7):562–571. doi:10.1016/j.biopsych.2012.04.024
19. Duman RS, Deyama S, Fogaça MV. Role of BDNF in the pathophysiology and treatment of depression: activity-dependent effects distinguish rapid-acting antidepressants. *Eur J Neurosci*. 2021;53(1):126–139. doi:10.1111/ejn.14630
20. Khan A, Shal B, Naveed M, et al. Matrine ameliorates anxiety and depression-like behaviour by targeting hyperammonemia-induced neuroinflammation and oxidative stress in CCl4 model of liver injury. *Neurotoxicology*. 2019;72:38–50. doi:10.1016/j.neuro.2019.02.002
21. Shi Y, Luan D, Song R, Zhang Z. Value of peripheral neurotrophin levels for the diagnosis of depression and response to treatment: a systematic review and meta-analysis. *Eur Neuropsychopharmacol*. 2020;41:40–51. doi:10.1016/j.euroneuro.2020.09.633
22. Kiuchi T, Lee H, Mikami T. Regular exercise cures depression-like behavior via VEGF-Flk-1 signaling in chronically stressed mice. *Neuroscience*. 2012;207:208–217. doi:10.1016/j.neuroscience.2012.01.023
23. Li X, Wu G, Han F, et al. SIRT1 activation promotes angiogenesis in diabetic wounds by protecting endothelial cells against oxidative stress. *Arch Biochem Biophys*. 2019;661:117–124. doi:10.1016/j.abb.2018.11.016
24. Huang X, Sun J, Chen G, et al. Resveratrol promotes diabetic wound healing via SIRT1-FOXO1-c-Myc signaling pathway-mediated angiogenesis. *Front Pharmacol*. 2019;10:421. doi:10.3389/fphar.2019.00421
25. Liu W, Yan H, Zhou D, et al. The depression GWAS risk allele predicts smaller cerebellar gray matter volume and reduced SIRT1 mRNA expression in Chinese population. *Transl Psychiatry*. 2019;9(1):333. doi:10.1038/s41398-019-0675-3
26. Ning HE, Ling JH, Linag G, Zhang Z, Wang YJ. [Effects of chaihu shugan powder on the cytoactivity of rat interstitial cells of Cajal and intracellular Ca^{2}+ Concentration]. *Zhongguo Zhong xi yi jie he za zhi Zhongguo Zhongxiyi jiehe zazhi*. 2016;36(9):1091–1096. Chinese.
27. Zhang S, Lu Y, Chen W, et al. Network pharmacology and experimental evidence: PI3K/AKT signaling pathway is involved in the antidepressive roles of Chaihu Shugan San. *Drug Des Devel Ther*. 2021;15:3425–3441. doi:10.2147/dddt.S315060
28. Liu MY, Yin CY, Zhu LJ, et al. Sucrose preference test for measurement of stress-induced anhedonia in mice. *Nat Protoc*. 2018;13(7):1686–1698. doi:10.1038/s41596-018-0011-z
29. Nishino T, Tamada K, Maeda A, et al. Behavioral analysis in mice deficient for GAREM2 (Grb2-associated regulator of Erk/MAPK subtype2) that is a subtype of highly expressing in the brain. *Mol Brain*. 2019;12(1):94. doi:10.1186/s13041-019-0512-x
30. Cryan JF, Mombereau C, Vassout A. The tail suspension test as a model for assessing antidepressant activity: review of pharmacological and genetic studies in mice. *Neurosci Biobehav Rev*. 2005;29(4–5):571–625. doi:10.1016/j.neubiorev.2005.03.009
31. Le-Niculescu H, Case NJ, Hulvershorn L, et al. Convergent functional genomic studies of ω-3 fatty acids in stress reactivity, bipolar disorder and alcoholism. *Transl Psychiatry*. 2011;1(4):e4. doi:10.1038/tp.2011.1

32. Qu M, Zhao J, Zhao Y, et al. Vascular protection and regenerative effects of intranasal DL-3-N-butylphthalide treatment after ischaemic stroke in mice. *Stroke Vasc Neurol*. 2021;6(1):74–79. doi:10.1136/svn-2020-000364
33. McCrary MR, Jiang MQ, Giddens MM, et al. Protective effects of GPR37 via regulation of inflammation and multiple cell death pathways after ischemic stroke in mice. *FASEB J*. 2019;33(10):10680–10691. doi:10.1096/fj.201900070R
34. Yu SP, Tung JK, Wei ZZ, et al. Optochemogenetic stimulation of transplanted iPS-NPCs enhances neuronal repair and functional recovery after ischemic stroke. *J Neurosci*. 2019;39(33):6571–6594. doi:10.1523/jneurosci.2010-18.2019
35. Yan GJ, Zhao HM, Hong X. LncRNA MACC1-AS1 attenuates microvascular endothelial cell injury and promotes angiogenesis under hypoxic conditions via modulating miR-6867-5p/TWIST1 in human brain microvascular endothelial cells. *Ann Transl Med*. 2021;8(14):876. doi:10.21037/atm-20-4915
36. Zeng W, Lei QL, Ma J, et al. Endothelial progenitor cell-derived microvesicles promote angiogenesis in rat brain microvascular endothelial cells in vitro. *Front Cell Neurosci*. 2021;15:638351. doi:10.3389/fncel.2021.638351
37. Burstein O, Doron R. The unpredictable chronic mild stress protocol for inducing anhedonia in mice. *J Vis Exp*. 2018;(140). doi:10.3791/58184
38. Han SK, Kim JK, Park HS, Shin YJ, Kim DH. Chaihu-Shugan-San (Shihosogansan) alleviates restraint stress-generated anxiety and depression in mice by regulating NF-κB-mediated BDNF expression through the modulation of gut microbiota. *Chin Med*. 2021;16(1):77. doi:10.1186/s13020-021-00492-5
39. Liu Q, Sun NN, Wu ZZ, Fan DH, Cao MQ. Chaihu-Shugan-San exerts an antidepressive effect by downregulating miR-124 and releasing inhibition of the MAPK14 and Gria3 signaling pathways. *Neural Regen Res*. 2018;13(5):837–845. doi:10.4103/1673-5374.232478
40. Li YH, Zhang CH, Wang SE, Qiu J, Hu SY, Xiao GL. [Effects of Chaihu Shugan San on behavior and plasma levels of corticotropin releasing hormone and adrenocorticotropic hormone of rats with chronic mild unpredicted stress depression]. *Zhong xi yi jie he xue bao*. 2009;7(11):1073–1077. Chinese. doi:10.3736/jcim20091110
41. Zhang H, Huang H, Song H, et al. Serum metabolomics reveals the intervention mechanism and compatible regularity of Chaihu Shu Gan San on chronic unpredictable mild stress-induced depression rat model. *J Pharm Pharmacol*. 2020;72(8):1133–1143. doi:10.1111/jphp.13286
42. Sun KH, Jin Y, Mei ZG, et al. Antidepressant-like effects of chaihu shugan powder () on rats exposed to chronic unpredictable mild stress through inhibition of endoplasmic reticulum stress-induced apoptosis. *Chin J Integr Med*. 2021;27(5):353–360. doi:10.1007/s11655-020-3228-y
43. Zhang R, Zhu X, Bai H, Ning K. Network pharmacology databases for traditional Chinese medicine: review and assessment. *Front Pharmacol*. 2019;10:123. doi:10.3389/fphar.2019.00123
44. Pantazatos SP, Huang YY, Rosoklija GB, Dwork AJ, Arango V, Mann JJ. Whole-transcriptome brain expression and exon-usage profiling in major depression and suicide: evidence for altered glial, endothelial and ATPase activity. *Mol Psychiatry*. 2017;22(5):760–773. doi:10.1038/mp.2016.130
45. Van Den Bossche MJA, Emsell L, Dols A, et al. Hippocampal volume change following ECT is mediated by rs699947 in the promotor region of VEGF. *Transl Psychiatry*. 2019;9(1):191. doi:10.1038/s41398-019-0530-6
46. Lehmann ML, Poffenberger CN, Elkahloun AG, Herkenham M. Analysis of cerebrovascular dysfunction caused by chronic social defeat in mice. *Brain Behav Immun*. 2020;88:735–747. doi:10.1016/j.bbi.2020.05.030
47. Mahajan GJ, Vallender EJ, Garrett MR, et al. Altered neuro-inflammatory gene expression in hippocampus in major depressive disorder. *Prog Neuropsychopharmacol Biol Psychiatry*. 2018;82:177–186. doi:10.1016/j.pnpbp.2017.11.017
48. Nuninga JO, Mandl RCW, Froeling M, et al. Vasogenic edema versus neuroplasticity as neural correlates of hippocampal volume increase following electroconvulsive therapy. *Brain Stimul*. 2020;13(4):1080–1086. doi:10.1016/j.brs.2020.04.017
49. Warner-Schmidt JL, Duman RS. VEGF as a potential target for therapeutic intervention in depression. *Curr Opin Pharmacol*. 2008;8(1):14–19. doi:10.1016/j.coph.2007.10.013
50. Whale R, Fialho R, Field AP, et al. Factor analyses differentiate clinical phenotypes of idiopathic and interferon-alpha-induced depression. *Brain Behav Immun*. 2019;80:519–524. doi:10.1016/j.bbi.2019.04.035
51. Minnema LA, Giezen TJ, Souverein PC, Egberts TCG, Leufkens HGM, Gardarsdottir H. Exploring the association between monoclonal antibodies and depression and suicidal ideation and behavior: a Vigibase Study. *Drug Safety*. 2019;42(7):887–895. doi:10.1007/s40264-018-00789-9
52. Zheng XW, Shan CS, Xu QQ, et al. Buyang huanwu decoction targets SIRT1/VEGF pathway to promote angiogenesis after cerebral ischemia/reperfusion injury. *Front Neurosci*. 2018;12:911. doi:10.3389/fnins.2018.00911
53. Leblond A, Pezet S, Cauvet A, et al. Implication of the deacetylase sirtuin-1 on synovial angiogenesis and persistence of experimental arthritis. *Ann Rheum Dis*. 2020;79(7):891–900. doi:10.1136/annrheumdis-2020-217377
54. Choi HK, Cho KB, Phuong NT, et al. SIRT1-mediated FoxO1 deacetylation is essential for multidrug resistance-associated protein 2 expression in tamoxifen-resistant breast cancer cells. *Mol Pharm*. 2013;10(7):2517–2527. doi:10.1021/mp400287p
55. Chen S, Zhao Z, Ke L, et al. Resveratrol improves glucose uptake in insulin-resistant adipocytes via Sirt1. *J Nutr Biochem*. 2018;55:209–218. doi:10.1016/j.jnutbio.2018.02.007
56. Wilhelm K, Happel K, Eelen G, et al. FOXO1 couples metabolic activity and growth state in the vascular endothelium. *Nature*. 2016;529(7585):216–220. doi:10.1038/nature16498
57. Jeon HH, Yu Q, Lu Y, et al. FOXO1 regulates VEGFA expression and promotes angiogenesis in healing wounds. *J Pathol*. 2018;245(3):258–264. doi:10.1002/path.5075
58. Ren B. FoxO1 transcriptional activities in VEGF expression and beyond: a key regulator in functional angiogenesis? *J Pathol*. 2018;245(3):255–257. doi:10.1002/path.5088
59. Abe-Higuchi N, Uchida S, Yamagata H, et al. Hippocampal sirtuin 1 signaling mediates depression-like behavior. *Biol Psychiatry*. 2016;80(11):815–826. doi:10.1016/j.biopsych.2016.01.009
60. Moore A, Beidler J, Hong MY. Resveratrol and depression in animal models: a systematic review of the biological mechanisms. *Molecules*. 2018;23(9):2197. doi:10.3390/molecules23092197
61. Segarra M, Aburto MR, Hefendehl J, Acker-Palmer A. Neurovascular interactions in the nervous system. *Annu Rev Cell Dev Biol*. 2019;35:615–635. doi:10.1146/annurev-cellbio-100818-125142